
Flames of Fuel Jets

30

DIFFUSION IN LAMINAR FLAME JETS¹

By H. C. HOTTEL² AND W. R. HAWTHORNE³

SUMMARY

The lengths and concentration patterns of flames from circular nozzles burning in free air have been determined over a wide range of velocities with several nozzle diameters and for various gases and primary air-gas ratios. As the nozzle velocity is increased from zero the flame, burning under conditions of diffusional mixing with air, increases in length until a transition occurs to turbulent combustion with a consequent change in flame length to a value which is substantially independent of further increase in velocity.

The present paper covers that portion of the data related to laminar jets and to transition phenomena. The progress of combustion is treated analytically, assuming that molecular diffusion is controlling and that the concentration of oxygen and fuel are zero at the flame interface. A relation is obtained between the time of flow of fuel gas to the flame tip and the proportion of nozzle fluid and air required for complete combustion as follows:

$$1/\theta_f = 4 \log_e \left(\frac{1 + a_t}{a_t - a_0} \right)$$

where $\theta_f = 4D_v t_f / D^2$

D_v = molecular diffusivity

t_f = time of flow from nozzle to flame tip

D = nozzle diameter

a_t = mols air/mol fuel gas for complete combustion

a_0 = mols air/mol fuel gas in nozzle fluid

¹ This paper is part of a thesis by W. R. Hawthorne submitted in 1939 to the Massachusetts Institute of Technology in partial fulfillment of the requirement for the ScD.

² Professor of Fuel Engineering, Massachusetts Institute of Technology.

³ Westinghouse Professor of Mechanical Engineering, Massachusetts Institute of Technology.

When the flame is short the time of flow is proportional to flame length, L ; for longer flames, the generalized flow-time for a given nozzle fluid, θ_f , should be a function of L/D , volumetric flow rate, Q , diffusivity, D_v , and the Grashof group which enters wherever the major force overcoming viscous drag is one of buoyancy. The actual relationship is established empirically from data on flames of carbon monoxide and of city gas. For flames longer than 6 inches, issuing from nozzles of diameters 0.125 to 0.82 inches, the following relation is suggested:

$$L = A \log Q\theta_f + B,$$

where A and B are constants depending only on the fuel gas and the primary air-fuel ratio.

Data on phenomena of transition from laminar to turbulent flow in the flame jet are also presented.

INTRODUCTION

Industrial gas-fired furnaces are characterized in a large number of cases by the mixing of the fuel gas and air streams in the combustion chamber of the furnace, so that the propagation of combustion is dependent on the rate of mixing of gas and air. A basic understanding of problems in combustion chamber and burner design, flame placement, and flame impingement thus requires the application of the concepts of mass transfer to the mixing process in flames. This mixing may occur in two ways:

- (1) Molecular diffusion. The mixing of two streams by molecular diffusion is relatively slow, and diffusion flames are used when a long, slow flame is desirable for the distribution of heat over large areas in the furnace. Such flames are used, for example, in rotary kilns.

(2) Turbulent mass transfer or eddy diffusion. In this case mass transfer is much more rapid than for molecular diffusion, since mixing occurs by the intermingling of micro-particles of fluid. Where high thermal output per unit of furnace volume is required, as in power plant operation, it is necessary to produce a turbulent flame.

In laminar flow, mixing is by molecular diffusion only, whereas in turbulent flow it is largely by eddy diffusion or convection, with the final homo-

point along the flame where breakdown of laminar flow occurs and a turbulent jet develops. The distance from the nozzle to the point where the turbulent brush begins may be termed the breakpoint length. Characteristic flame length and breakpoint length curves have been obtained for various nozzles and fuel gases; one such set of curves is shown in figure 1. The appearance of the diffusion and turbulent flames is demonstrated by the sketches in figure 2. As the nozzle velocity increases from zero there is at first an almost pro-

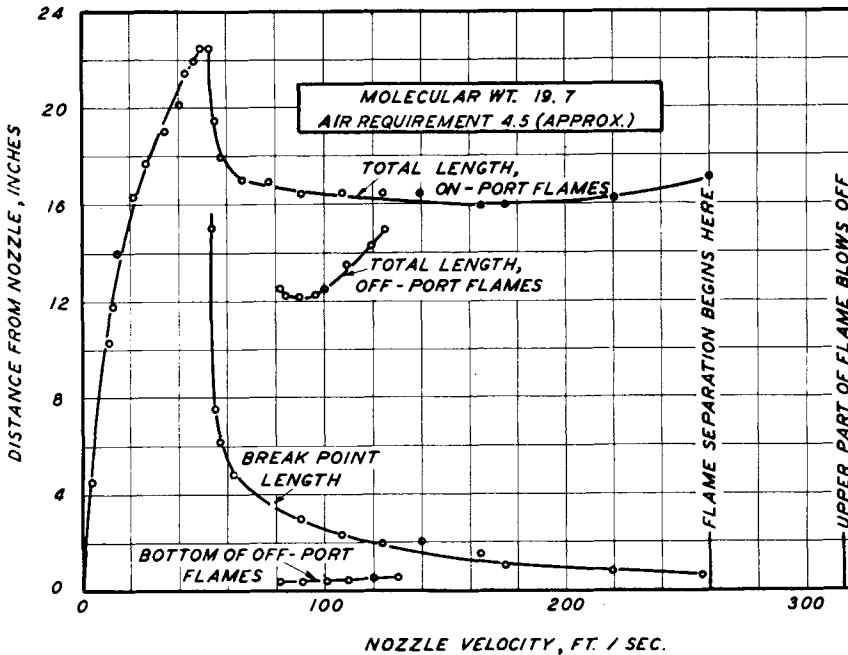


FIG. 1. Effect of nozzle velocity on flame length of city gas flames with no primary air; $\frac{1}{8}$ inch diameter nozzle; from Gaunce (5).

geneity being attained by molecular diffusion between small-scale eddies.

The flame from a circular nozzle provides a simple illustration of the difference between burning and mixing in laminar and in turbulent flow. When fuel gas discharges at velocities below a critical value from the nozzle into quiet air of large extent, the flow of gas is laminar, and the mixing of gas and air occurs by molecular diffusion in a thin flame surface which is fixed in space. As the nozzle velocity is increased the diffusion flames increase in length until a critical velocity is reached and the tip of the flame becomes unsteady and begins to flutter. With further increase in velocity this unsteadiness develops into a noisy turbulent brush of flame starting at a definite

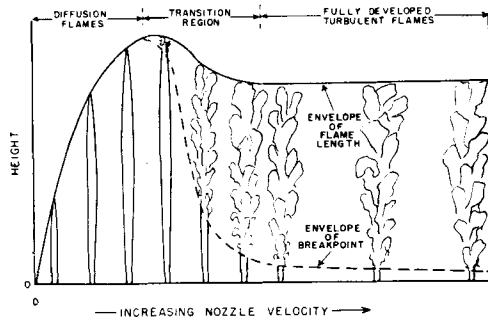


FIG. 2. Progressive change in flame type with increase in nozzle velocity.

portional increase in flame length, and at any velocity in this region the flame is sharp-edged and constant in shape. When a sufficiently high

velocity is reached (fourth sketch) the tip of the flame changes in character, and a slight brush forms. With further increase in nozzle velocity the point at which the flame "breaks" moves toward the nozzle, and the tip of the flame moves toward a new height different from that of the longest pure diffusion flame (in the present example, shorter). At a nozzle velocity corresponding to the seventh sketch the break-point has approached quite close to the nozzle, and substantially the whole flame has become turbulent. Further increase in velocity affects the total flame length and break-point very little, but flame noise continues to increase and flame luminosity continues to decrease. The flame finally blows off the port at a velocity of 50–1000 feet per second, depending on the gas, flame pilot, and nozzle size.

A study of these flames was undertaken with the object of applying the concepts of mass transfer to mixing in the flames. In this paper only the work on diffusion flames and diffusion flame breakdown is discussed; two later papers cover the work on turbulent flames and their representation by liquid models.

DIFFUSION FLAMES

Measurements of the length of city gas diffusion flames issuing into quiet air from a circular nozzle were made by Rembert (1). Cuthbertson (2) made similar measurements, but does not identify the fuel gas he used.

The shape and characteristics of diffusion flames in which the velocity of the mixing streams was extremely low were studied by Burke and Schumann (3). They gave a simplified mathematical analysis of the diffusion process which enabled flame shapes to be determined theoretically. Theoretical predictions were in good agreement with their experimental results.

EXPERIMENTAL APPARATUS

A circular burner nozzle to which were led known quantities of gas (and in some cases primary air) was situated at the bottom of a vertical cylindrical furnace of relatively large dimensions, figure 3. A known quantity of secondary air was introduced at the bottom of the furnace through straighteners and screens, so that a uniform, steady and slow flow of air was provided for the combustion and scavenging. Three sizes of burner port were used, $\frac{1}{8}$ inch, $\frac{3}{16}$ inch, and $\frac{1}{4}$ inch inside diameter (fig. 4). To minimize rotation and turbulence in the issuing gas, straighteners and screens were

placed in the pipe before the gas stream was contracted down to one-ninth of its cross-sectional area. The contraction was followed by a straight section, six port diameters long, which was long enough to prevent the issuing jet from wobbling and short enough to prevent excessive development of turbulent velocity components, or to cause a noticeable departure from uniform velocity over the cross section of the stream.

The measurement of gas and primary air flow was carried out by orifice meters with an accuracy of $1\frac{1}{2}$ percent. Two scales placed on either side of the flame enabled the position of a given point in the flame relative to the burner port to be measured to within ± 2 mm. In the region of transition from laminar to turbulent jet the break-

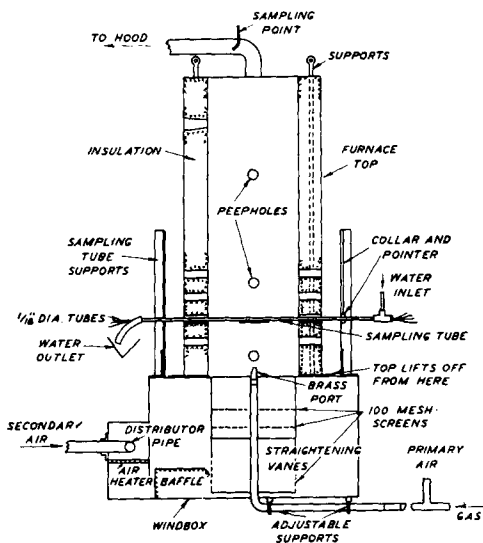


FIG. 3. Experimental furnace.

point tended to be somewhat unstable, so that the reproducibility of the measurement was within ± 0.5 cm. in this region. Reproducibility was considerably better at higher velocities, where the breakpoint was more stable. The flame lengths were reproducible to within ± 0.5 cm. Flame length measurements were made with the furnace top removed. Gas sampling in the flame was done with the furnace top in place as described below.

To obtain samples of gas from the flames a water-cooled sampling tube was used, figure 5. A thin brass wedge was arranged to project downwards from a horizontal water-cooled tube. Samples were withdrawn from the thin edge of the

wedge through seven stainless steel tubes, .025 inch inside diameter, which were soldered to $\frac{1}{16}$ inch o.d. copper tubing inside the water-cooled tube. The seven sampling points were situated half an inch below the center of the water-cooled tube of $\frac{3}{8}$ inch diameter; and there was no observable disturbance to the gas flow up to the sampling point.

in the study of turbulent flames (to be described in another paper).

DIFFUSION PROCESS IN THE FLAME

The process of diffusion occurring in a flame of hydrogen leaving a port $\frac{1}{4}$ inch diameter at a velocity of 108 ft./sec.⁴ is illustrated in figure 6,

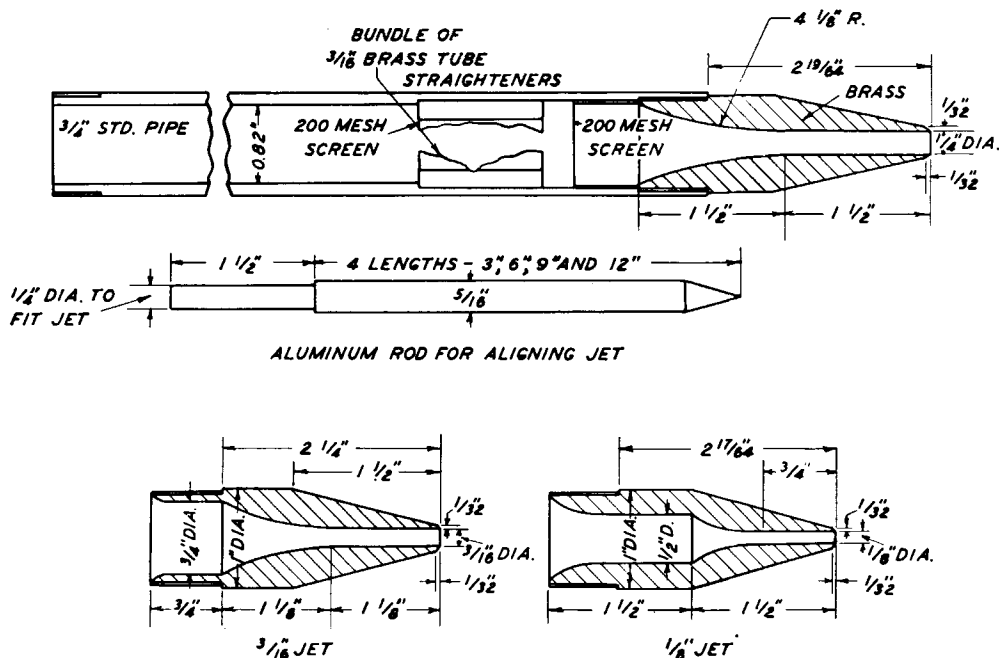


FIG. 4. Details of rounded nozzles.

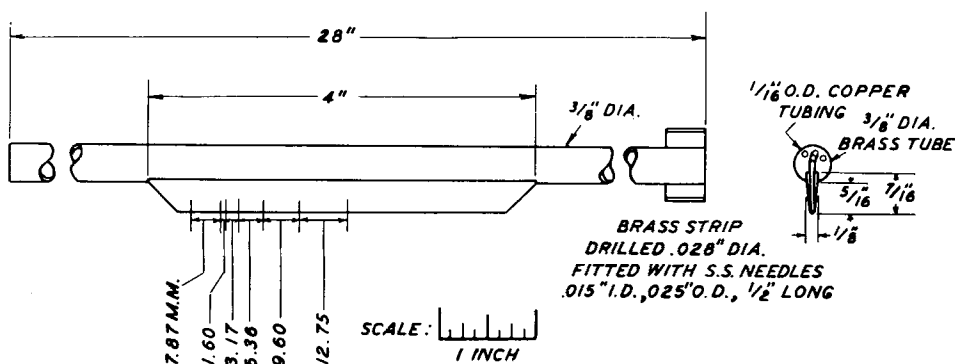


FIG. 5. Water-cooled sampling tube.

The samples were drawn out simultaneously and stored in sample bottles to await analysis. The time taken to obtain one batch of seven samples was approximately ten minutes; and during this time the gas and air flows were maintained steady under the action of pressure-regulating valves. This same apparatus was used to a limited extent

in which the analyses of samples taken across the flame at three different distances from the port are presented. In spite of a slight unsteadiness, and the consequent appearance of oxygen in sam-

⁴ Nozzle velocity is calculated at room temperature and pressure.

ples from the center of the flame,⁵ the data provide adequate illustration of the generalized picture, figure 7. The fuel molecules are diffusing outward to the flame surface where they meet oxygen

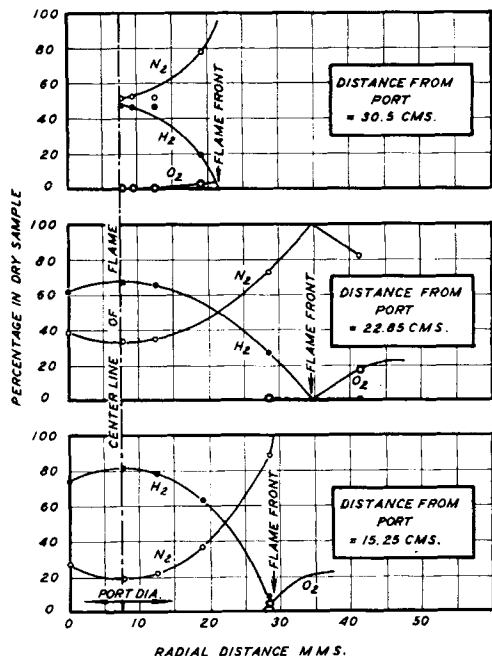


FIG. 6. Gas composition in hydrogen diffusion flame; $\frac{1}{4}$ inch diameter nozzle; nozzle velocity 108 ft./sec.

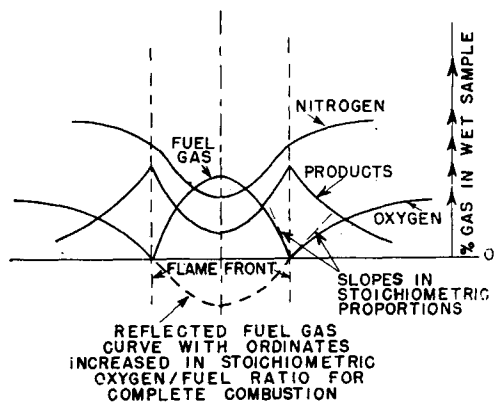


FIG. 7. Simplification of diffusion process in a typical flame.

molecules diffusing inwards from the outside air. Neither fuel nor oxygen molecules actually pass through the flame envelope or reaction zone. The

⁵ Due to the flame occasionally being blown away from the sampling point so that air passes it at some time during the ten minute period of sampling.

combustion products which are formed at this zone diffuse both inward and outward. Nitrogen passes through the flame surface, diffusing inward.

The rigorous analysis of the diffusion process in the flame would be extremely complicated, but by following Burke and Schumann's (3) suggestion, simplification of the problem is possible if it is assumed: (a) that the combustion reaction takes place instantaneously and with no change in number of mols and (b) that the temperature and diffusivities of the gases are everywhere constant and equal. The system may then be divided into two zones, one inside the flame envelope and one outside. In each zone either gas or oxygen is diffusing towards and disappearing at the flame front, while nitrogen plus the products of combustion, which may be considered as one gas, enter each zone from the flame front where their concentration is unity. In each zone, therefore, unsteady state diffusion of two gases is occurring and the rate of diffusion of each is proportional to its concentration gradient. Reflection of the curve for fuel gas concentration, figure 7, in the horizontal axis, and scaling of the ordinates of the reflected curve in the ratio, mols of oxygen required for complete combustion of the gas per mol of fuel gas, gives a curve which has the same slope as the oxygen curve at the flame front and which, therefore, runs smoothly into the oxygen curve. The continuous curve for oxygen and equivalent fuel gas, expressed as "negative oxygen," may then be used as if it represented the concentration of one gas in a system consisting of two diffusing gases.

In terms of the above simplified diffusion system the gas everywhere consists of two components, "oxygen" and nitrogen-plus-combustion-products, and the sum of their separate mol fractions (called concentration here) everywhere equals unity. The concentration of "oxygen" in the sample, designated by c , is defined as the mols of oxygen in the sample minus the mols of oxygen required to burn completely any unburned gas in the sample, all divided by the sum of the mols of nozzle fluid and surrounding fluid required to produce the sample. (It is to be noted that in the diffusion flame, where no oxygen occurs on one side of the flame surface and no unburned fuel gas on the other side, either the oxygen or the fuel term appears in the numerator of c , but not both.) Expression of c in terms of air/fuel ratios is desirable. Let a_0 be the primary air/fuel gas molal ratio in the nozzle fluid, and a_i the stoichiometric ratio or theoretical ratio for perfect combustion. Then c at the nozzle

is $0.21(a_0 - a_t)/(1 + a_0)$; c at the flame tip and everywhere else on the flame surface is 0; and c in the ambient air is 0.21.

With the generalized "oxygen" content c of a fuel-air system defined, it is desirable to express concentration dimensionlessly by defining the term C_m as

$$C_m = \frac{(c \text{ at time to flow from nozzle to any specified point along the axis of the flame}) - (c \text{ at infinite time})}{(\text{initial } c \text{ in nozzle fluid}) - (c \text{ at infinite time})}$$

It is seen that C_m is the unaccomplished fractional change in concentration, expressed as a fraction of the total possible change from the value at the nozzle to the ultimate value along the flame axis at infinity. The value of C_m at the flame tip, called C_f , is given by

$$C_m \text{ at flame tip} \equiv C_f = \frac{0 - .21}{.21(a_0 - a_t) - .21} = \frac{1 + a_0}{1 + a_t} \quad (1)$$

For example, consider a methane flame burning with no primary air. Since one volume of methane requires 2 volumes of oxygen for complete combustion, the equivalent "oxygen" concentration in the pure methane at the port is -2.0 , and varies along the flame axis from -2.0 through 0 at the flame tip on to $+0.21$ at an infinite distance. The total possible change is 2.21, and the fractional change out to the flame tip is $2/2.21 = 0.905$. The unaccomplished fractional change is $1 - 0.905 = 0.095$; this is C_f .

The problem of diffusion in the simplified open-flame system just described is treated in the Appendix. It leads to a relation between the quantities, generalized concentration C_m and generalized time θ , defined as follows:

$$\theta = 4D_v t / D^2, \quad (2)$$

where t = elapsed time for gas to flow from nozzle to point where concentration is C_m ,

D_v = molecular diffusivity coefficient for the system,

D = nozzle diameter.

The relation is

$$C_m = 1 - e^{-1/4\theta} \quad (3)$$

The value of θ_f , or θ at the flame tip, comes from a substitution from (1) into (3) to obtain

$$\frac{1 + a_0}{1 + a_t} = 1 - e^{-1/4\theta_f} \quad (4)$$

from which

$$\theta_f = \frac{1}{4 \ln [(1 + a_t)/(a_t - a_0)]} \quad (5)$$

The next problem is to relate the time factor, θ , to the distance along the flame. It is desired to know t_f , the time of flow to the flame tip. Actually the flame length, L , was measured, not t_f ; hence θ_f must be expressed in terms of L . Certain assumptions have therefore to be made as to the change of gas velocity v , along the length of the flame so that θ_f may be evaluated from the expression

$$\theta_f = \frac{4D_v t_f}{D^2} = \frac{4D_v}{D^2} \int_0^{t_f} dt = \frac{4D_v}{D^2} \int_0^L \frac{dx}{v} \quad (6)$$

where v = the gas velocity at a distance x from the nozzle; i.e. the solution of equation 6 involves the determination of the relationship between v and x . The gas velocities used are very small and are decreased by viscous drag and increased as a result of the density difference between the gas stream and its surroundings.

Problems involving this balance of viscous drag versus buoyancy are known to involve a dimensionless parameter due to Grashof, namely $(Gr) = D^3 \rho^2 \beta g \Delta t / \mu^2$, where ρ , β , g , μ and Δt are respectively density, temperature coefficient of expansion, gravitational acceleration, viscosity, and temperature difference. The velocity v at any point x along the flame axis should then be expressible in the dimensionless form

$$\frac{v}{V} = f_1 \left(\frac{D^3 \rho^2 \beta g \Delta t}{\mu^2}, \frac{x}{D}, a_0 \right), \quad (7)$$

where V is the nozzle velocity, and a_0 is introduced because of its possible effect on combustion rate and consequently on the temperature pattern and resultant buoyancy. Equation 6 may be written as

$$\theta_f = \frac{4D_v}{VD^2} \int_0^L \frac{dx}{v/V} \quad (6a)$$

The volumetric flow rate, Q , equals $\pi VD^2/4$. Making this substitution in equation 6a, substituting v/V from equation 7, one obtains

$$\frac{Q\theta_f}{\pi D_v} = \int_0^L \frac{dx}{f_1(Gr, a_0, x/D)} = f_2(L, D, Gr, a_0) \quad (8)$$

If attention is focused on a single primary air/fuel ratio a_0 then, since all the fuel gases on which data are here available have about the same theoretical combustion temperature and produce combustion products of about the same molecular weight, the only quantity in the Grashof number which is

monoxide flames are plotted as $Q\theta_f$ versus flame length L for different diameters and fixed values of primary air/fuel ratio a_0 . It will be noted that these data, covering a 7-fold range of values of port diameter D , fit curves of the form

$$L = A \log_{10} Q\theta_f + B \quad (10)$$

where A and B are independent of velocity and port diameter.

Further evidence to support the generalization that L depends on D and V only as they affect

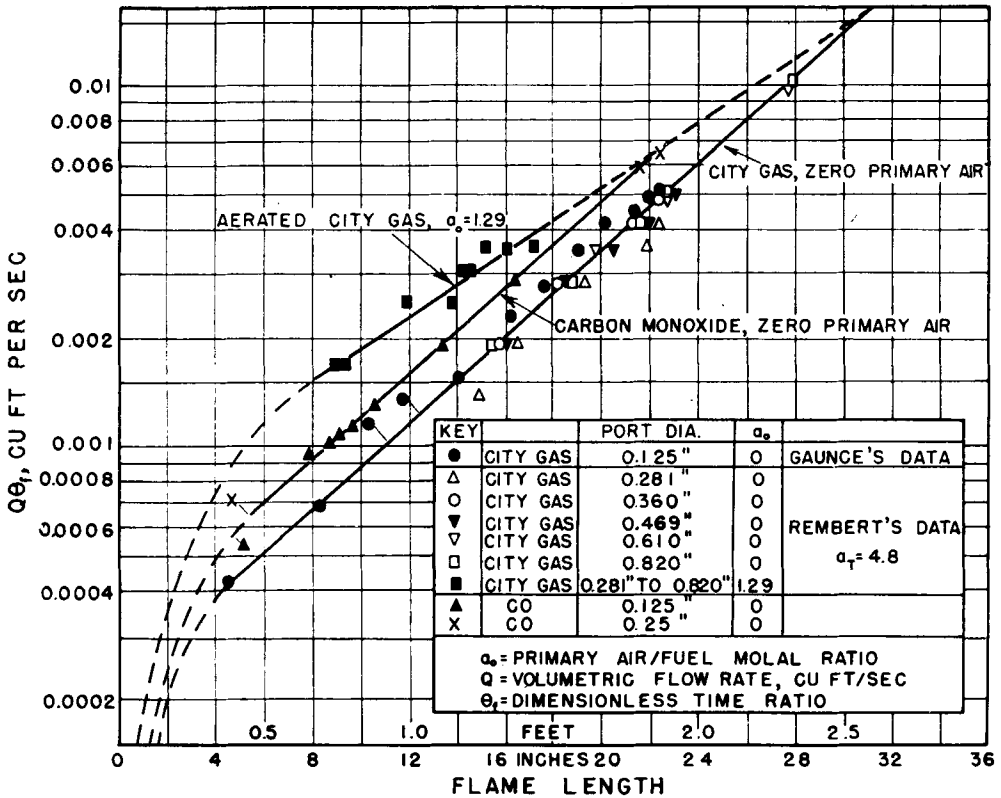


FIG. 8. Correlation of data on lengths of diffusion flames.

variable in these experiments is the diameter D . In addition, D_v will be constant. Consequently, equation 8 becomes

$$Q\theta_f = f_3(L, D, a_0) \quad (9)$$

However, when experimental data are studied, L and Q being measured and θ_f being calculated from equation 5, L is found to be a unique function of $Q\theta_f$, and *not* dependent on the diameter D of the nozzle. This is illustrated in figure 8, where some of Rembert's (1) data, the data of Gaunce (5) on city-gas flames, and the author's data for carbon

flow-rate Q comes from other data of Rembert (1) given in table 1. At fixed values of Q and a_0 , a 3-fold variation in nozzle diameter is seen to produce but a minor variation in flame length at constant Q .⁶

The dependence of L on $Q\theta_f$ alone, and not on D , suggests the need for imposing a limitation on the general treatment that led to equation 9. If in equation 7 the Grashof number and x/D enter

⁶ There is some suggestion in the data, however, that at high primary air-fuel ratios ($a_0 = 2$) the flame length may decrease somewhat as nozzle diameter increases, at constant Q .

as a product term $(Gr)^{1/3}(x/D)$, then D disappears from equation 7, and consequently from equation 8, and equation 9 becomes

$$Q\theta_f = f_4(L, a_0), \tag{11}$$

a relation seen to be consistent with the experimentally established relation 10.

Although equation 10 appears to be a satisfactory form of the more general equation 11 in the range covered by the data, no data were obtained at flame lengths less than about 5 inches. (The experiments had been designed primarily for the study of turbulent flames, and the gas-measuring equipment was unsatisfactory at the extremely low velocities necessary to produce short diffusion flames.) In the region of extremely low nozzle velocity it is unlikely that v/V varies much from

Values of the constants A and B of equation 10 are given in table 2, for L and Q having the dimensions, feet and cu. ft. per sec. at room temperature and pressure. It is to be noted that un-aerated carbon monoxide has the same value of A as un-aerated city gas.

Rembert (1) obtained an empirical equation for flame length, by plotting and cross-plotting his data, in the form

$$L' = f(a_0) \log_{10} V + \phi(a_0) \log_{10} D' + \psi(a_0) \tag{13}$$

where L' and D' are in inches and V is in ft./sec., and f , ϕ , and ψ are three different functions of a_0 . The present analysis suggests that this should be reducible to the form of equation 10. This is possible if $\phi(a_0)$ is double $f(a_0)$. It will be seen

TABLE 1
Data of Rembert on city-gas flame lengths
(Each line of data corresponds to constant flow rate Q)

	Flame length, inches, when nozzle diameter, inches, is:					Average length, inches	Percent spread around average
	0.28	0.36	0.47	0.61	0.82		
$Q = 0.0055$ $\left\{ \begin{array}{l} a_0 = 0.5 \\ 1.0 \\ 2.0 \end{array} \right.$		20.1	20.5	20.0	20.3	20.2	± 1
		16.5	16.0	15.1	—	15.3	+5, -4
		11.6	10.9	10.2	9.9	9.0	+12, -13
$Q = 0.0021; a_0 = 0.5$	10.9	10.5	11.7	10.0	—	10.8	+8, -7
$Q = 0.0032; a_0 = 0$	22.4	21.3	22.1	—	21.4	21.8	+3, -2
$Q = 0.0034; a_0 = 1.29$	—	9.5	9.4	8.9	—	9.3	+2, -4

Air requirement of city-gas used, $a_r = 4.8$; M.W. = 14.7.

unity before the flame tip is reached; hence equation 6a leads to the relation

$$L = \frac{VD^2\theta_f}{4D_v} = \frac{Q\theta_f}{\pi D_v} \tag{12}$$

This approach of L to proportionality to Q at low values of L is in accordance with the experimental results of Burke and Schumann (3). The data are inadequate to permit accurate determination of the point at which transition begins to occur from equation 10 to equation 12, but figures 1 and 8 are helpful. All the experimental data points appearing on the diffusion-flame portion of the curve of figure 1 fit fairly well the straight-line relation appearing on figure 8. Prediction by equation 10 of flame lengths less than six inches is probably unsafe.

TABLE 2
Values of A and B in equation, $L = A \log_{10} Q\theta_f + B$

Gas	a_0	A	B
City gas	0	1.39	5.09
	1.29	1.87	5.93
Carbon monoxide	0	1.39	4.91

In calculation of θ_f , $a_t = 2.38$ for carbon monoxide; for city gas it varies with composition from 4.3 to 4.8.

from table 3 containing values of the functions of a_0 in Rembert's equation that $\phi(a_0)$ is of the right order, except for $a_0 = 0.5$. A comparison of values of L predicted by Rembert's equation with his own experimental data indicates that his recommended values of $f(a_0)$ and $\phi(a_0)$ at $a_0 = 0.5$

were poorly chosen and predict an effect of diameter not supported by his data in table 1; and that a better set of values do satisfy the condition $\phi(a_0) = 2f(a_0)$. It appears, then, that the present recommended equation 10 fits the data at least as well as the more complicated equation 13.

Use of equation 10 to predict city gas diffusion-flame lengths at other values of primary air than those given in table 2 may be desirable. Rembert's data given in table 1 have been used to

TABLE 3
Functions of a_0 in Rembert's equation

a_0	$f(a_0)$	$\phi(a_0)$	$\psi(a_0)$
0	17.6	33.9	25.2
0.5	23.3	32.6	18.9
1	23.5	43.0	14.0
2	21.6	39.0	8.6

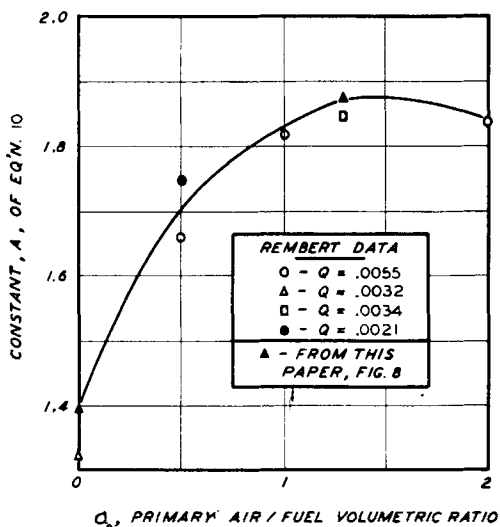


Fig. 9. Variation, with a_0 , of constant "A" of equation 10.

calculate, for his various values of a_0 , the values of A which would make equation 10 fit. The results of the calculation are presented in figure 9 as A versus a_0 . On the same plot appear the two values of A obtained by weighting all data appearing in figure 8. The curve drawn through these two best established points is recommended for use until more data become available. It is not now known whether this curve, which fits both city gas and carbon monoxide at zero primary air, fits the second gas at other values of a_0 .

DIFFUSION FLAME BREAKDOWN

Although the experiments described above were designed primarily for study of mixing in flames, the associated transition phenomena from laminar to turbulent flames were so striking that some measurements of break-point lengths were made in the apparatus. These measurements were also required in the study of turbulent flames because in some instances the length of flame from nozzle to breakpoint was an appreciable fraction of the total flame length and it was important to have measurements of the point at which turbulent mixing commenced. It is to be understood that the conditions for study of the phenomenon were not controlled to the extent accepted as being necessary for the elimination of unknown turbulence so important in the study of laminar flow instability.

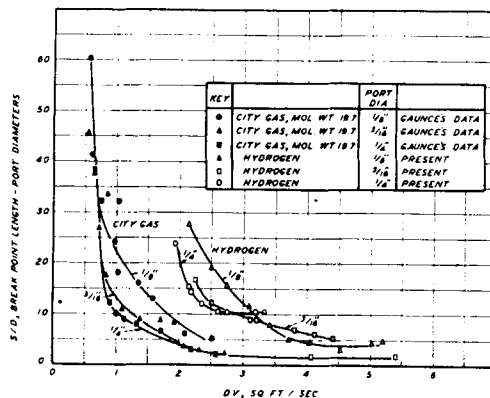


Fig. 10. Breakpoint lengths, hydrogen and city-gas flames (non-premix).

The furnace top was removed for these measurements, and in some cases the secondary air was turned on to steady the flames. (Its velocity was approximately 0.2 ft./sec.) Where observation of the breakpoint was difficult because of low flame luminosity, direct visual observation was supplemented by examination of the shadow produced by shining an intense light from a single point-source through the flame onto a white screen.

The characteristic variation of break-point length with nozzle velocity is apparent in figure 1 and in figure 10, where data on hydrogen and city gas flames are plotted. At some critical port velocity in the region of transition from diffusion to turbulent flame the breakpoint starts at the flame tip (see figs. 1 and 2) and moves down towards the port rapidly with increasing port velocity. At higher velocities breakpoint becomes

relatively constant. The breakpoint was found to be perfectly stable, and there was no random breakdown from laminar to turbulent flow caused by disturbances in the surrounding air, except with the very long diffusion flames from small ports in the region of the critical velocity; such flames could be affected by clapping of the hands.

Experimental work on turbulent jets of air and gas reported in the literature does not include reference to this break-point phenomenon. It is evident from a study of this work that the transition from laminar to turbulent flow occurred very close to the port. In work to be reported in a later paper on turbulent mixing in liquid jets it was found, however, that the break-point behavior of a small liquid jet was very similar to that shown in figures 1 or 10. This suggests that the phenomenon is related to fluid flow rather than to combustion, requiring interpretation in the case of flames in terms of the local physical factors such as viscosity and density in the flame.

As it is of importance to be able to predict in practice the region in which transition from laminar to turbulent flow occurs, all the data available have been presented in Appendix II. The Reynolds numbers given there are in terms of the viscosity and density of the nozzle fluid at room temperature. That this is not the correct basis for correlation is clear from the scatter of critical values obtained, and from the effect of varying nozzle and surrounding fluid densities and viscosities indicated in the results from liquid jets. Figure 11 has, however, been constructed as a guide to indicate approximately the region in which transition may be expected to occur. The difficulties normally associated with experimental and theoretical study of laminar flow instability even in simple aerodynamic systems combined with the unknown variation in physical factors due to local heat release make any further study of the present data fruitless.

A phenomenon of interest and possible practical importance connected with the break-point behavior was observed during the experimental work. Over a certain range of port velocity it was possible to obtain two stable but different flames. The first, or on-port flame, is that already described, figure 1, with ignition commencing at the port. In the second, ignition occurred some short distance above the port, and the flame was everywhere turbulent and shorter than the first flame by a distance almost equal to the break-point length, figure 1. This latter off-port flame could

also be obtained at high port velocities, if a small pilot flame was used to locate the ignition point. The striking reduction of total flame length attendant on the later initiation of combustion is probably associated with the effect of local Reynolds number on break-point length. If break-point length increases with decreasing port velocity (see fig. 1) it should similarly increase with increasing local viscosity. The hot mantle of flame around the jet at the base of the on-port flame produces a high viscosity which delays initiation of turbulent

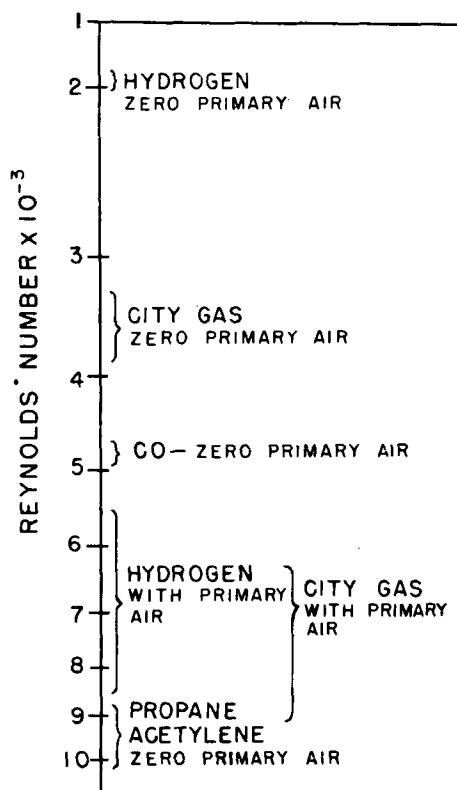


FIG. 11. Values of Reynolds number (cold) at which transition from diffusion to turbulent flames commences.

mixing. Accordingly, the total space required for combustion is less when ignition is delayed to permit early transition to turbulent flow. City gas off-port flames were less luminous than on-port flames, due probably to the early aeration of the flame which reduced the thermal decomposition normally occurring when gas is heated in the absence of air.

ENGINEERING APPLICATION

Although the relationships for flame length established are based on limited data, they may be

used to estimate the space requirement for diffusion-flame combustion under conditions of free access of atmospheric air. As an example of use, let the problem at hand be the estimation of flame length when natural gas is burning in an unrestricted air supply, issuing at a velocity of ten feet per second from a quarter-inch port. To ensure this is outside the transition region the Reynolds number is required. Assuming the gas is pure methane, the viscosity at 60°F. is 108×10^{-6} poises or 7.25×10^{-6} fps units; the density at 60°F. is $(16/359) \times (492/520) = 0.0422$ lb./cu.ft.; whence the Reynolds number is $10 \times (0.0422/7.25 \times 10^{-6}) \times (1/48) = 1,210$, i.e. well below the critical range. The volume flow rate Q is $10(\pi/4)(\frac{1}{4})^2 \times 144 = 0.0342$ cu. ft./sec. The primary air/fuel ratio a_0 is zero. The theoretical volumetric air/fuel ratio for complete combustion, a_t , based on the assumption that the fuel is pure methane, is $2 \times (100/21) = 9.52$. The value C_f , from equation 4, is $(1 + 0)/(1 + 9.52) = 0.095$. From equation 3, $C_f = 1 - e^{-1/4\theta_f}$, or $\theta_f = 1/(-4 \ln(1 - C_f)) = 1/(-4 \times 2.303 \times \log_{10} 0.905) = 2.7$. From figure 9 or table 2, A and B are estimated as 1.4 and 5.0. Then

$$\begin{aligned} L &= A \log_{10} (Q\theta_f) + B \\ &= 1.4 \log_{10} (0.0342 \times 2.7) + 5.0 \\ &= 2.15 \text{ ft.} = 26 \text{ inches.} \end{aligned}$$

Use of this method of estimating diffusion flame length must at present be restricted to those fuel gases for which A and B can be estimated; these constants are presumably dependent on gas density and air requirement a_t .

APPENDIX I

For the cylindrical system described in the text the diffusion equation is:

$$\frac{\partial c}{\partial t} = D_v \left(\frac{\partial^2 c}{\partial y^2} + \frac{1}{y} \frac{\partial c}{\partial y} \right) \quad (1)$$

where c = the concentration of oxygen or the negative oxygen equivalent of the combustible gas (defined more completely in the text),

y = radial distance from the axis of the flame,

t = elapsed time,

D_v = molecular diffusivity coefficient for the system.

Putting $Y = 2y/D$, where D = diameter of the

port, and assuming D_v is constant, equation 1 becomes

$$\frac{\partial C}{\partial \theta} = \frac{\partial^2 C}{\partial Y^2} + \frac{1}{Y} \frac{\partial C}{\partial Y} \quad (2)$$

where $\theta = 4D_v t/D^2$ and

$$C = \frac{\begin{array}{l} (c \text{ at time to flow from port to any} \\ \text{specified point in the flame)} \\ - (c \text{ at infinite time)} \\ \text{(initial } c \text{ in nozzle fluid)} \\ - (c \text{ at infinite time)} \end{array}}$$

The relation 2 is dimensionless and has the boundary conditions (see fig. 7):

$$\frac{\partial C}{\partial Y} = 0 \quad \text{when } Y = 0 \text{ and } Y = \infty;$$

and when $\theta = 0$, $C = 1$ from $Y = 0$ to ± 1 and $C = 0$ from $Y = \pm 1$ to $\pm \infty$.

A solution of equation 2 is

$$C = \int_0^\infty e^{-\lambda^2 \theta} \cdot J_0(\lambda Y) \cdot J_1(\lambda) \cdot d\lambda, \quad (3)$$

where J_0 and J_1 are zero- and first-order Bessel functions, respectively.

This satisfies the boundary conditions for $\partial C/\partial Y$. Also, when $\theta = 0$,

$$\begin{aligned} C &= \int_0^\infty J_0(\lambda Y) J_1(\lambda) \cdot d\lambda = 1 \text{ when } Y^2 < 1 \\ &= \frac{1}{2} \text{ when } Y^2 = 1 \\ &= 0 \text{ when } Y^2 > 1 \end{aligned}$$

(see page 78 of ref. 4).

When $Y = 0$, $J_0(\lambda Y) = 1$ and the axial concentration is given by:

$$C_m = \int_0^\infty e^{-\lambda^2 \theta} J_1(\lambda) \cdot d\lambda \quad (4)$$

Now

$$\begin{aligned} J_1(\lambda) &= \frac{\lambda}{2} - \frac{(\lambda/2)^3}{2!} + \frac{(\lambda/2)^5}{2!3!} \\ &+ \dots \frac{(-1)^r (\lambda/2)^{2r+1}}{r!(r+1)!} \end{aligned} \quad (5)$$

and since

$$\int_0^\infty e^{-\lambda^2 \theta} \lambda^{2r+1} d\lambda = \frac{r!}{2\theta^{r+1}} \quad (6)$$

$$\begin{aligned} C_m &= \sum_0^\infty \frac{(-1)^r}{(r+1)! (4\theta)^{r+1}} \\ &= 1 - e^{-1/4\theta} \end{aligned} \quad (7)$$

APPENDIX II

Experimental data on transition from diffusion to turbulent flames.

- (1) Hydrogen; zero primary air; viscosity 90×10^{-6} poises at 20°C .; nozzle gas density relative to air .0693.

Nozzle diameter	Nozzle Reynolds number (room temperature and pressure)		
	when s/D is		
	25	10	5
$\frac{1}{8}$ inch	2160	3230	3640
$\frac{3}{16}$ inch	—	2800	4600
$\frac{1}{4}$ inch	1910	2600	—

- (2) Hydrogen; with primary air

Nozzle diameter, inch	$a_0 = 0.2$ $\mu = 131 \times 10^{-6}$ poises		$a_0 = 0.4$ $\mu = 147 \times 10^{-6}$					
	Relative density	Re when s/D is		Relative density	Re when s/D is			
		Large	25		Large	100	50	25
$\frac{1}{8}$.222	7380	8340	.33	8270	—	9630	—
$\frac{3}{16}$.224	—	7800	.335	6200	—	6350	—
$\frac{1}{4}$.250	5550	6690	.350	7630	—	—	7700

$a_0 = 0.6$
 $\mu = 156 \times 10^{-6}$

Relative density	Re when s/D is			
	Large	100	50	25
.403	7850	8650	—	—
.422	6180	—	7480	11,500
.432	6400	—	—	8,250

- (3) City gas; zero primary air; viscosity 140×10^{-6} poises at 20°C .; nozzle gas density relative to air = 0.69.

Nozzle diameter	Re when s/D is:			
	Large	25	10	5
$\frac{1}{8}$ inch	3720	5740	11,700	16,700
$\frac{3}{16}$ inch	3380	4280	8,260	11,400
$\frac{1}{4}$ inch	3980	4380	6,630	10,900

- (4) City gas; with primary air; $\frac{1}{4}$ inch nozzle.

a_0	Relative density	Viscosity, poises	when s/D is	
			50	25
.54	.715	150×10^{-6}	6,200	8,300
.84	.762	153×10^{-6}	8,340	10,350
1.61	.832	158×10^{-6}	—	12,000

- (5) Carbon monoxide; zero primary air; viscosity 170×10^{-6} poises; nozzle gas density relative to air 0.967; $\frac{1}{4}$ inch diameter nozzle.

when s/D is large, Re = 4,750
25, Re = 5,350
10, Re = 7,050

- (6) Propane; zero primary air; viscosity 82×10^{-6} poises; density relative to air 1.49; $\frac{1}{8}$ inch nozzle diameter.

when s/D is 25, Re = 10,400

- (7) Acetylene; zero primary air; viscosity 93×10^{-6} poises; density relative to air 0.9; $\frac{1}{8}$ inch nozzle diameter.

when s/D is large, Re = 8,900
25, Re = 12,500
10, Re = 33,100

- (8) Cold air jets. Data from experiments with $\frac{1}{8}$ inch and $\frac{1}{4}$ inch nozzles indicate that s/D is 10 or less when the Reynolds number is 2,500.

- (9) Liquid jets; nozzle diameter .041 inch.

	Density relative to surrounding fluid						
	1	1	1	1.06	1	0.9	0.82
Nozzle fluid viscosity, centipoises	1.16	1.46	2.61	1.54	1.54	1.54	1.54
Surrounding fluid viscosity, centipoises	1.05	1.46	1.05	1.54	1.54	1.54	1.54
when s/D is							
10, Re =	1400	2000	520	1340	1940	1900	1940
5, Re =	2440	3200	2050	2860	3100	3060	—

TABLE OF NOMENCLATURE

- A, B = constants in equation 10
 a_0 = mols. primary air/mol. fuel gas
 a_t = air required for complete combustion of one mol of fuel gas
 c = concentration of oxygen or the negative oxygen equivalent of the combustible gas
 C = (c at a given point. — c at infinite time)(initial c — c at infinite time)
 D, D' = nozzle diameter, feet and inches, respectively
 D_s = coefficient of molecular diffusivity, ft^2/sec .
 g = acceleration due to gravity
 Gr = Grashof's number = $D^3 \rho_2 \beta g \Delta t / \mu_2$
 J_0, J_1 = Bessel functions of zero- and first-order
 L, L' = flame length, feet and inches, respectively
 Q = rate of flow from nozzle, ft^3/sec . (room temp. and press.)
 s = distance from break-point to port, ft.
 t = elapsed time, sec.
 v = gas velocity along the axis of the flame, ft/sec .

V = nozzle velocity (room temp. and press.),
ft./sec.

x = distance from nozzle along axis of the flame,
ft.

y = radial distance from axis of the flame, ft.

$Y = 2y/D$

$\theta = 4D_t/D^2$

ρ = density of gas

β = coefficient of expansion of gas

Δt = temperature difference

μ = viscosity of gas

Subscripts m and f = value of C , θ , and t on the flame
axis and at the flame tip.

REFERENCES

1. REMBERT, E. W., AND HASLAM, R. T.: *Ind. and Eng. Chemistry*, *17*, 1236 (Dec. 1925).
2. CUTHBERTSON, J.: *Journal Society Chemical Ind. Trans.*, *50*, 451-457 (1931).
3. BURKE, S., AND SCHUMANN, T.: *Ind. Engineering Chemistry*, *20*, 998-1009 (1928).
4. GRAY, MATTHEWS, AND MACROBERT: *A Treatise on Bessel Functions and Their Applications to Physics*. Macmillan (1931).
5. GAUNCE, H.: Unpublished research at M.I.T., 1939.

MIXING AND COMBUSTION IN TURBULENT GAS JETS¹

By W. R. HAWTHORNE,² D. S. WEDDELL,³ AND H. C. HOTTEL⁴

ABSTRACT

Visible flame lengths and concentration patterns have been obtained in turbulent jets of flame formed by combustible gas issuing from circular nozzles into stagnant air. The nozzle velocities were above those which, in a previous paper, were found necessary to insure that the mixing should be turbulent. As a basis for analysis of the data a simplified treatment is presented for mixing of nozzle and ambient fluids in a vertical jet. The simplifying assumption of constant velocity and composition in a cross-section normal to the axis of flow is combined with a force-momentum balance, continuity, and the perfect gas laws to obtain a relation between mean concentration and jet spread. The relation allows for initial difference in density of nozzle and ambient streams, density variation due to combustion, and buoyancy. The qualitative agreement between the analysis and the experimental data on visible flame lengths and axial concentration patterns indicates plainly that the process of mixing resulting from the momentum and buoyancy of the jet is the controlling factor in determining progress of the combustion. For free flames in which the effects

of buoyancy are small (high nozzle velocity, small diameter) the analysis leads to the following simple relation for the length of free turbulent flame jets:

$$L/D = \frac{5.3}{C_T} \sqrt{\frac{T_F}{\alpha_T T_N} \left[C_T + (1 - C_T) \frac{M_S}{M_N} \right]}$$

- where L = visible flame length
 D = nozzle diameter
 T_F = adiabatic flame temperature, absolute
 T_N = absolute temperature of nozzle fluid
 M_S, M_N = molecular weights of surrounding and nozzle fluids, respectively
 C_T = mol fraction of nozzle fluid in the unreacted stoichiometric mixture
 α_T = mols of reactants/mols products, for the stoichiometric mixture.

It is to be noted that fuel gas flow rate is no factor, as long as it is great enough to produce a turbulent jet. Although data for testing this relation covered the small range of port diameter of 0.12 to 0.30 inches, a wide variety of fuels was studied, including propane, acetylene, hydrogen, carbon monoxide, city gas, mixtures of carbon dioxide with city gas, and mixtures of hydrogen with propane. Turbulent flame lengths varying from 40 to 290 nozzle diameters are predicted with average and

¹ From theses submitted in partial requirement for the degree of Sc.D. by W. R. Hawthorne, 1939, and by D. S. Weddell, 1941.

² Westinghouse Professor of Mechanical Engineering, Massachusetts Institute of Technology.

³ At present with Monsanto Chemical Company.

⁴ Professor of Fuel Engineering, Massachusetts Institute of Technology.